JOURNAL OF ENVIRONMENTAL SCIENCES 68 (2018) 91–99

Available online at www.sciencedirect.com

ScienceDirect

www.elsevier.com/locate/jes

JES JOURNAL OF ENVIRONMENTAL SCIENCES

www.jesc.ac.cn

Mercury flows in large-scale gold production and implications for Hg pollution control

Qingru Wu[1,2], *Shuxiao Wang*[1,2,*], *Mei Yang*[1,2], *Haitao Su*[3], *Guoliang Li*[1,2], *Yi Tang*[1,2], *Jiming Hao*[1,2]

1. *State Key Joint Laboratory of Environment Simulation and Pollution Control, School of Environment, Tsinghua University, Beijing 100084, China*
2. *State Environmental Protection Key Laboratory of Sources and Control of Air Pollution Complex, Beijing 100084, China*
3. *College of Electromechanical Engineering, Qingdao University of Science and Technology, Qingdao 266061, China*

ARTICLE INFO

Article history:
Received 24 January 2017
Revised 16 March 2017
Accepted 17 March 2017
Available online 30 March 2017

Keywords:
Large-scale gold production
Mercury
Flow analysis
Emission characteristics

ABSTRACT

Large-scale gold production (LSGP) is one of the five convention-related atmospheric mercury (Hg) emission sources in the *Minamata Convention on Mercury*. However, field experiments on Hg flows of the whole process of LSGP are limited. To identify the atmospheric Hg emission points and understand Hg emission characteristics of LSGP, Hg flows in two gold smelters were studied. Overall atmospheric Hg emissions accounted for 10%–17% of total Hg outputs and the Hg emission factors for all processes were 7.6–9.6 kg/ton. There were three dominant atmospheric Hg emission points in the studied gold smelters, including the exhaust gas of the roasting process, exhaust gas from the environmental fog collection stack and exhaust gas from the converter of the refining process. Atmospheric Hg emissions from the roasting process only accounted for 16%–29% of total emissions and the rest were emitted from the refining process. The overall Hg speciation profile (gaseous elemental Hg/gaseous oxidized Hg/particulate-bound Hg) for LSGP was 34.1/57.1/8.8. The dominant Hg output byproducts included waste acid, sulfuric acid and cyanide leaching residue. Total Hg outputs from these three byproducts were 80% in smelter A and 84% in smelter B. Our study indicated that previous atmospheric Hg emissions from large-scale gold production might have been overestimated. Hg emission control in LSGP is not especially urgent in China compared to other significant emission sources (*e.g.*, cement plants). Instead, LSGP is a potential Hg release source due to the high Hg output proportions to acid and sludge.

Introduction

To reduce global mercury (Hg) pollution caused by anthropogenic Hg emissions, the international community approved the *Minamata Convention on Mercury* (UNEP, 2013a). Large-scale gold production (LSGP, also known as industrial gold production) is one of the most significant anthropogenic Hg emission sources and also one of the five convention-related emission sources in the convention (UNEP, 2013a). China is the largest gold producing country in the world (CGS, 2015). Therefore, understanding the Hg emission characteristics of LSGP is important for Hg pollution control in China.

Due to the lack of information on Hg emission characteristics in LSGP, the emission factor of 790 kg/ton derived from artisanal and small-scale gold mining (ASGM) was firstly applied to estimate Hg emission from China's LSGP (Dai et al., 2003; Jiang,

* *Corresponding author*. E-mail: shxwang@tsinghua.edu.cn (Shuxiao Wang).

http://dx.doi.org/10.1016/j.jes.2017.03.029

2004; Streets et al., 2005; Wu et al., 2006). However, considering that Hg input to LSGP is mainly from gold ores while pure Hg is also used as a dominant raw material in ASGM (Dai et al., 2003; Jiang, 2004; Yang et al., 2016), compiling an inventory for LSGP by using the emission factor for ASGM overestimated LSGP's emissions. The emission factors were then reduced to the range of 25–500 kg/ton in later studies without experimental specifications (Pacyna et al., 2006, 2010; AMAP/UNEP, 2008; Pirrone et al., 2010; Streets et al., 2011; Tian et al., 2015; UNEP, 2013b; Wu et al., 2016; Zhang et al., 2015). The above-mentioned Hg emission factors were subject to high uncertainty due to the lack of knowledge on the variation of the Hg concentration in gold concentrates and the detailed gold production process. The global Hg assessment report estimated that the Hg emission factor from LSGP was 55 kg/ton based on the assumption that air pollution control devices (APCDs) were not applied at LSGP (AMAP/UNEP, 2013). However, a recent field experiment indicated that sufficient APCDs were applied for air pollutant control in China's LSGP (Yang et al., 2016). The overall synergistic Hg removal efficiency of APCDs for the two-stage roasting process reached as high as 96% (Yang et al., 2016). The tested emission factor for the roasting process was in the range of 0.5–1.7 kg/ton (Gao et al., 2016; Yang et al., 2016). However, Hg emission characteristics and Hg flows in the refining process were not tested in these two studies.

This study presents a comprehensive investigation on Hg flows in all the gold production processes including roasting, cyanide leaching, and refining in two of China's gold smelters. Emission points and characteristics were systematically studied to generate technology-based emission factors. Overall Hg mass balances were analyzed to identify the final fate of Hg in the LSGP. The results from this study can be applied in both the emission inventory and Hg flow analyses, and will provide a scientific foundation for Hg pollution control in China.

1. Experimental

1.1. Tested plants

Two gold smelters were tested in this study, which were denoted as smelter A and smelter B. Both of these smelters extracted refined gold from ores by using heap leaching roasting technology, a widely used technology in China's LSGP. Overall gold production processes in the two smelters included roasting, cyanide leaching, and the refining process (Fig. 1). In addition, the APCDs of the sampled company include acid plants with double contact and double absorption towers (APD) and a flue gas absorption tower (FGA). These APCDs represent the major flue gas processing techniques.

The roasting process can be divided into one-stage and two-stage roasting processes, which were used in smelter A and smelter B, respectively. Gold concentrates were ground to make a mixed pulp. Mixed pulp was roasted in a roaster (650°C) for 3 hr. in smelter A. Two roasters were applied to roast the pulp for a total of 1.5 hr. in smelter B. The temperature of the first roaster was approximately 500–550°C and the roasting time was approximately 0.5–1 hr. The rest of the time was used to roast the residue in the second roaster (550–620°C). Calcine was produced and further disposed in the cyanide leaching process. In both smelters, flue gas from roasters was cleaned by a series of devices before being emitted to air, including dust collectors (DCs), flue gas scrubbers (FGSs), an electrostatic demister (ESD), APD, and FGA. In the APD system, the SO_2 was transformed into SO_3 using a V_2O_5-catalyst and then absorbed *via* dilute sulfuric acid. In the APD tower, the SO_2 was absorbed *via* H_2O_2 solution. The DCs in smelter A included a cooler and two-stage cyclone (CYCs) while DCs in smelter B were a combination of cooler, CYC and electrostatic precipitator (ESP). FGSs in smelter A consisted of Venturi and packing towers, whereas an additional foam tower was installed between the Venturi and packing towers in smelter B. Air pollutants were removed to different wastes/byproducts, including dust, waste acid, sulfuric acid, and spray waste acid. Dust and a limited amount of sulfuric acid were also input to the cyanide leaching process with calcine, whereas the rest of the wastes/byproducts were released out of the gold production system.

In the cyanide leaching process, the calcine and dust were firstly dissolved in the acid liquid to remove impurities. Then, the solid materials were separated and used to generate a pregnant solution with gold in NaCN solution. Solid impurities from the solution were released out of the system as cyanide residue. The pregnant solution was used to extract gold sludge by applying the zinc powder replacement method, and the barren liquid was simultaneously removed out of the system.

In the refining process, the gold sludge was firstly leached in nitric acid. The nitrate leaching liquid was used to produce silver and the nitrate leaching sludge was dissolved in aqua regia solution to separate gold from other solid impurities. The solid impurities from the aqua regia solution were smelted in the converter. The gold-bearing liquid was reduced to make gold powder and some part of the reduction liquid was released out of the system. In the above stages, fogs from nitrate leaching, gold separating, and reduction stages were collected and cleaned with an FGA. In the converter smelting stage, flue gas was firstly cooled and then cleaned with a two-stage FGA. Dust and dust sludge were produced during the flue gas cleaning process.

1.2. Sampling and analysis methods

1.2.1. Sampling method

Solid and liquid samples collected are listed in Table 1. These samples were collected according to corresponding standards, which were described in detail in our previous studies (MEP, 2002; Wu et al., 2015b; Zhang et al., 2012a). Flue gas sampling locations are shown in Fig. 1. Flue gas samples were collected by using the Ontario Hydro method (OH method) when the SO_2 concentrations in the flue gas were less than 1000 ppm (ASTM, 2002). For locations where SO_2 concentrations were higher than 1000 ppm, the revised OH method was adopted (Wu et al., 2015b; Zhang et al., 2012b). Compared to the OH method, the revised OH method replaced the 1 mol/L KCl impinger solution with 1 mol/L KOH and the concentration of H_2O_2 was increased from 1% to 3%. A detailed description of both the OH method and revised OH method were given in our previous studies (Wu et al., 2015b).

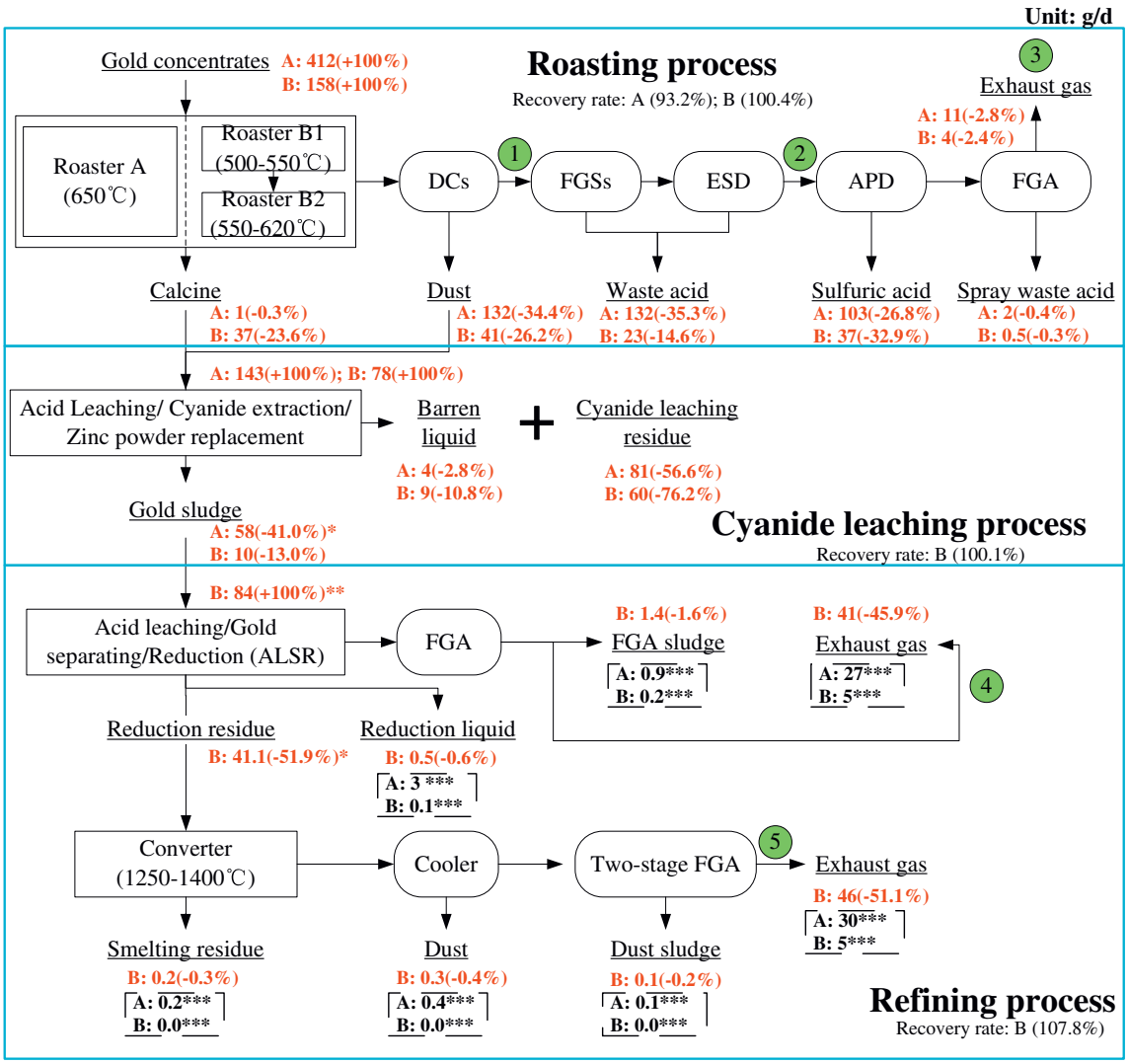

Note:
DC: Dust collectors, including cooler (A and B), cyclone (A), electrostatic precipitator (B);
FGS: Flue gas scrubber, including Venturi (A and B), foam tower (B), packing tower (A and B);
ESD: Electrostatic demister; FGA: Flue gas absorption tower;
*: Calculated by mass balance method;
**: Daily produced gold sludge was collected for 3-7 days before refining;
***: Hg amount in the daily produced gold sludge of cyanidation-leaching process were distributed to the refining process according the tested distribution proportion in smelter B
-: Not produced in corresponding smelter.
(1) Flue gas sampling points.

Fig. 1 – Chart of Hg flows in the studied gold production processes.

1.2.2. Collection and analysis method

The collected solid samples were dried and crushed to 100 mesh and then analyzed using a Lumex 915 M + PYRO attachment. This equipment applied the U.S. EPA 7473 method (US EPA, 1998) and its detection limit was 0.5 mg/ton. The liquid samples and impinger solutions were analyzed immediately after sampling according to the U.S. EPA method 7470A (US EPA, 1994) with a F732-VJ intelligent mercury analyzer. This equipment used cold vapor atomic absorption spectrophotometry (CVAAS) and had a detection limit of 0.05 mg/L.

1.2.3. Hg release rate and Hg removal efficiency

The Hg release rate in the roaster or converter can be calculated by the following equation.

$$\gamma_i = \left(1 - \frac{C_{i,residue} \times M_{i,residue}}{C_{i,input} \times M_{i,input}}\right) \times 100\% \quad \text{(E1)}$$

The Hg removal efficiency η of APCD j, which is defined as the fraction of Hg captured by the device, can be calculated as follows.

$$\eta_j = \frac{C_{captured,j} \times M_{captured,j}}{C_{captured,j} \times M_{captured,j} + C_{outlet,j} \times M_{outlet,j}} \times 100\% \quad \text{(E2)}$$

Table 1 – Hg concentrations and productions/consumptions of samples.

Process	Samples	Smelter A				Smelter B			
		Concen.	Unit	Pro./Con.	Unit	Concen.	Unit	Pro./Con.	Unit
Roasting process	Gold concentrates	5490	ng/g	75	ton/day	543	ng/g	290	ton/day
	Calcine	20	ng/g	50	ton/day	179	ng/g	209	ton/day
	Dust (from DCs-cooler)	2800	ng/g	7	ton/day	/	/	/	/
	Dust (from DCs-CYC 1)	282	ng/g	11	ton/day	/	/	/	/
	Dust (from DCs-CYC 2)	13,660	ng/g	8	ton/day	/	/	/	/
	Dust (from DCs-ESP and cooler)	/	/	/	/	1787	ng/g	23	ton/day
	Flue gas after ESP	N.T	N.T	220	km^3/day	365	$\mu g/m^3$	609	km^3/day
	Waste acid (from FGSs)	127	ng/g	1040	ton/day	/	/	/	/
	Waste acid (from ESD)	357	ng/g	10	ton/day	/	/	/	/
	Waste acid (from FGSs + ESD)	/	/	/	/	5	ng/g	37	ton/day
	Acid slag (from FGSs + ESD)	/	/	/	/	396,552	ng/g	0.058	ton/day
	Flue gas after ESD	577	$\mu g/m^3$	220	km^3/day	212	$\mu g/m^3$	609	km^3/d
	Sulfuric acid	2800	ng/g	37	ton/day	197	ng/g	264	ton/day
	Spray waste liquid	15	ng/g	129	ton/day	25	ng/g	20	ton/day
	Exhaust gas from roasting process	50	$\mu g/m^3$	220	km^3/day	6	$\mu g/m^3$	609	km^3/day
Cyanide leaching process	Barren liquid	11	ng/g	364	ton/day	8	ng/g	1160	ton/day
	Cyanide leaching residue	1168	ng/g	69	ton/day	258	ng/g	232	ton/day
	Gold sludge	N.T.	N.T.	N.T.	N.T.	97,470	ng/g	0.11	ton/day
Refining process	Gold sludge	N.T	N.T	N.T	N.T	97,470	ng/g	1	ton/day
	FGA sludge	N.T	N.T	N.T	N.T	11,826	ng/g	0.012	ton/day
	Exhaust gas from environmental fog collection stack	N.T	N.T	N.T	N.T	6	$\mu g/m^3$	7200	km^3/day
	Reduction solution	N.T	N.T	N.T	N.T	242	ng/g	2	ton/day
	Dust (from cooler)	N.T	N.T	N.T	N.T	11,374	ng/g	0.03	ton/day
	Dust sludge	N.T	N.T	N.T	N.T	23,892	ng/g	0.06	ton/day
	Exhaust gas from converter	N.T	N.T	N.T	N.T	4	$\mu g/m^3$	12,000	km^3/day
	Smelting slag	N.T	N.T	N.T	N.T	4084	ng/g	0.06	ton/day

Note: "Concen." is the abbreviation of concentration; "Pro./Con." is the abbreviation of production/consumption; "/"means that no sampling at this site or no such materials; "N.T." means no test; "U.L." means that the concentration of the sample is under limit.

where $C_{residue}$ (ng/g) and $M_{residue}$ (ton/day) are Hg concentration and production of residue from roaster or converter *i*. C_{input} (ng/g) and M_{input} (ton/day) are Hg concentration and consumption of raw materials to roaster or converter. $C_{captured}$ (ng/g) and $M_{captured}$ (ton/day) are the Hg concentration and production of the materials produced by APCD *j*. C_{outlet} ($\mu g/m^3$) and M_{outlet} (km^3/day) are the Hg concentration of flue gas and gas flow rate at the outlet of the APCDs.

1.3. Quality assurance and quality control (QA/QC)

Before sampling, bottles used to collect solid and liquid samples and sampling lines of the flue gas sampling system were cleaned in the lab by immersion in a 10% HNO_3 (V/V) bath for 24 hr, followed by repeated rinses in Milli-Q grade water (18.2 MΩ cm). The flue gaseous Hg sampling system was calibrated and a leak test was performed. During the sampling period, all solid and liquid samples were collected one time per day and at least three samples per time. For gaseous samples, more than three parallel samplings under stable operating conditions were conducted to ensure the validity of the results. During the analysis period, each solid/liquid sample was analyzed at least 3 times to obtain parallel results, with a relative standard deviation of less than 10%. The certified reference material of Zn/Pb ores (certified reference for the component analysis of rich Zn/Pb ores, GBW07165, supplied by the National Research Center for CRMs of China) was used as an external standard. For gaseous Hg absorbed in the impinger solutions, Hg concentrations in all of the reagents should be under the detection limit. Hg mass in the last KCl (or KOH) impinger for gaseous oxidized Hg (Hg^{2+}) and the last $KMnO_4$/H_2SO_4 impinger for gaseous elemental Hg (Hg^0) absorption should be less than 15% of total Hg^{2+} and Hg^0 mass, respectively.

2. Results and discussion

2.1. Hg concentrations in the samples

2.1.1. Hg concentrations in the solid/liquid samples

Hg concentrations in the solid and liquid samples are shown in Table 1. The average Hg concentrations in the concentrates consumed in smelter A and B were 5490 and 543 ng/g. Gold concentrates were the dominant source of Hg input. The fuel for the roasting stage is coal and oil, but the mercury contribution of the fuel is so low that it can be neglected. This was proved in our previous study (Wu et al., 2015a). In the roasting process, the Hg concentration of calcine from smelter A (20 ng/g) was lower than that of smelter B (179 ng/g) due to the higher roasting temperature and longer roasting time in smelter A. In smelter A, the highest Hg concentration (13,660 ng/g) was identified in the dust from the cyclone. However, acid slag was the byproduct with the highest Hg concentration (396,552 ng/g) in smelter B.

The higher Hg concentration in the dust from smelter A may be caused by a higher Hg concentration in the gold concentrates consumed. The Hg concentrations in the sulfuric acid produced in both smelters were less than 10 μg/g, the criterion of best sulfuric acid quality in China (GAQSIQ, 2014). Hg concentrations in the spray waste liquid from smelter A and B were 15 and 25 ng/g. In the cyanide leaching process, cyanide leaching residue and gold sludge were two byproducts with high Hg concentrations. Hg concentrations in the barren liquid were limited. In the refining process, the Hg concentration in the reduction solution of smelter B was 242 ng/g, much lower than the concentrations in the solid samples (dust, dust sludge, and FGA sludge). However, although the Hg concentrations in all solid samples were higher than 1000 ng/g, their production levels were quite small.

2.1.2. Hg concentration and speciation in the flue gas

For smelter A, Hg concentrations in the flue gas after ESD (point A2) reached 577 μg/m^3, which were higher than the concentrations at point B2. In addition, the particulate-bound Hg (Hg_p) proportion in point A2 reached 25%, while the proportion was only 4% in point B2. The higher Hg_p proportion at point A2 was mainly caused by its lower dust removal efficiency. In smelter A, two CYCs with 95% dust removal efficiency were applied, whereas both a CYC and ESP (dust removal efficiency >99%) were used in smelter B. Considering the high dust ratio of more than 60% in the flue gas from the roasters, the higher amount of dust in the flue gas of smelter A will provide much more surface to adsorb Hg and cause a higher Hg_p proportion. In the exhaust gas from the roasting process (point A3 and B3), Hg concentrations were 50 μg/m^3 in smelter A and 6 μg/m^3 in smelter B. The Hg speciation profiles ($Hg^0/Hg^{2+}/Hg_p$) for the exhaust roasting gas of smelter A and smelter B were 10.3/89.5/0.2 and 49.0/42.7/8.3. The result of two-stage roasting in smelter B is very similar to Yang et al. (2016) study.

There were two stacks for exhaust gas emissions, including the environmental fog collection stack (point B4) and stack for exhaust gas from the converter (point B5). Hg concentrations in both of the kinds of exhaust gases were less than 10 μg/m^3. Hg^{2+} was the dominant Hg speciation in the exhaust gases, accounting for 61% at point B4 and 83% at point B5. The Hg speciation profile ($Hg^0/Hg^{2+}/Hg_p$) for exhaust refining gas in smelter B was 18.6/71.8/9.6. When atmospheric Hg emissions from both the roasting and refining processes were considered, the overall Hg speciation profile ($Hg^0/Hg^{2+}/Hg_p$) for LSGP was 34.1/57.1/8.8, which was quite different from the derived profile of 80/15/5 applied in previous emission inventories (Streets et al., 2005; Wu et al., 2006; Zhang et al., 2015).

2.2. Hg flows in the studied smelters

Hg flows in the two studied smelters are shown in Fig. 1. In the roasting process, Hg was input with gold concentrates and distributed to calcine, dust, waste acid, sulfuric acid, spray waste acid, and exhaust gas. During the roasting, approximately 0.3% and 23.6% of Hg was left in the calcine, indicating that 99.7% and 76.4% of Hg was released to flue gas in smelters A and B (Table 2). Considering that Hg in certain chemical speciation types in the gold concentrates required high temperature (more than 780°C) for Hg evaporation (Yang et al., 2016), the higher Hg release rate in smelter A may be caused by its higher roasting temperature and longer roasting time.

Hg released into flue gas was captured to different by products due to the synergistic Hg removal efficiencies of the APCDs. The overall Hg removal efficiencies of APCDs in the roasting process were 97.1% in smelter A and 96.2% in smelter B. The Hg removal efficiencies of DCs in smelter A and B were 34.7% and 35.7%, respectively. In smelter A, the DCs included a cooler and two-stage CYCs, whereas the second stage CYC was replaced with an ESP in smelter B. Generally, the dust removal efficiencies of CYC and ESP are approximately 85% and 98% (Yang et al., 2016). Besides, the ESP is effective in removing dust with smaller diameter, which provides more surfaces for Hg adsorption (Wu et al., 2015b; Yang et al., 2016). Thus, the Hg removal efficiency of the DCs in smelter B was higher than that in smelter A. The Hg removal efficiencies of FGS + ESD were 53.2% in smelter A and 35.7% in smelter B. The Hg_p concentration after FGS + ESD (point A2) in smelter A reached 141 μg/m^3 (Fig. 2). Considering the washing effect to Hg_p of FGS + ESD, the Hg_p concentrations at point A1 will be much higher than 141 μg/m^3. However, the Hg_p concentrations in smelter B before FGS + ESD (point B1) were only 72 μg/m^3. Thus, the higher Hg removal efficiencies of FGS + ESD in smelter A may be caused by its higher Hg_p concentrations. In the APD and FGA, the higher Hg removal efficiencies in smelter A were mainly due to higher concentrations of both total Hg and oxidized Hg (sum of Hg^{2+} and Hg_p).

Table 2 – Hg release rates of furnaces and removal efficiencies of APCDs (%).

Processes	Furnace/APCDs		Smelter A	Smelter B
Roasting process	Roaster	Release rate	99.7	76.4
	DCs	Removal efficiency	34.7	38.9
	FGS + ESD	Removal efficiency	53.2	35.7
	APD	Removal efficiency	88.8	35.7
	FGA	Removal efficiency	15.4	11.1
	All APCDs	Removal efficiency	97.1	96.2
Refining process	Converter	Release rate	N.T	99.7
	FGA	Removal efficiency	N.T	3.3
	Cooler	Removal efficiency	N.T	0.6
	Two-stage FGA	Removal efficiency	N.T	0.2

DCs: dust collectors; FGS: flue gas scrubber; ESD: electrostatic demister; FGA: flue gas adsorption; N.T. means no test; APCDs: air pollution control devices.

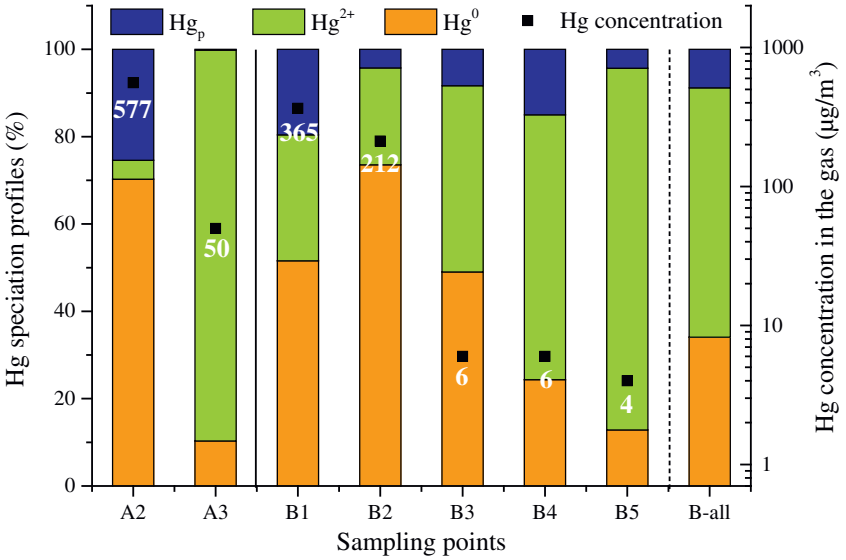

Fig. 2 – Hg speciation profiles and Hg concentrations in the gas; the A and B represents smelter A and smelter B; the number 1–5 represents the sampling position in Fig. 1.

Due to the impact of the APCDs, approximately 14.6%–35.3% and 0.4%–0.3% of Hg was removed to waste acid and spray waste acid in the roasting process. The subsequent waste acid disposal process will further distribute this part of Hg to different wastewater slugs. Hg in the sulfuric acid accounted for 26.8%–32.9% of total Hg output in the roasting process. The further utilization of the sulfuric acid should pay attention to potential Hg pollution to other environmental media. For example, fertilizer which uses sulfuric acid as a raw material will be a potential source of soil Hg pollution. Hg remaining in the calcine and dust accounted for approximately 34.7% in smelter A and 49.8% in smelter B. This part of Hg was input to the cyanide leaching process. In this process, approximately 56.6%–76.2% of Hg was left in the cyanide leaching residue. Metals (gold, silver, copper, lead, *etc.*) in the cyanide leaching residue were recovered in some smelters, but parts of the cyanide leaching residue were still left in the tailing pond. Thus, potential environmental risk from cyanide leaching residue should also draw attention. Total Hg output to barren liquid was only 2.8% in smelter A and 10.8% in smelter B. The remaining Hg was output from the cyanide leaching process as gold sludge, accounting for approximately 41% and 13% of the Hg outputs of this process in smelter A and B, respectively.

The gold sludge was used to extract refined gold in the refining process. In the acid leaching/gold separation/reduction (ALSR) stage, a large amount of Hg was evaporated to gas. In the converter refining stage, the Hg release rate in the converter reached 99.7% due to the high smelting temperature of 1250–1400°C. Thus, nearly all Hg in the gold sludge was released to gas. Although a cooler and FGA were also used for flue gas cleaning, the Hg removal efficiencies were only 0.6% for the cooler and 0.2%–0.6% for FGA, much lower than that in the roasting process. In the refining process, although Hg concentrations in the exhaust gas of B4 and B5 were only 6 and 4 μg/m^3, the gas flow reached 7200 and 12,000 km^3/day, approximately 12 and 20 times the flow in the exhaust roasting gas. Thus, atmospheric Hg emissions reached 87 g/d during the studied period. In this process, atmospheric Hg emissions accounted for 97% of total Hg outputs, leaving the rest in the dust, reduction liquid, and dust sludge.

2.3. Overall Hg mass balances

Considering that the daily production of gold sludge was not enough for refining, the refining processes were generally operated for 3–7 days per month after collecting enough gold sludge. Thus, to estimate the overall Hg mass balances, the Hg amount in the daily produced gold sludge of cyanide leaching process was distributed to the refining process according the measured distribution proportion in smelter B. The overall Hg outputs in the studied smelters are shown in Fig. 3. Hg recovery rates were 96% in smelter A and 91% in smelter B, which were in the range of acceptable accuracies (Wang et al., 2016; Wu et al., 2015b; Zhang et al., 2012b).

Although the amounts of Hg output to different byproducts or air were quite different in the two studied smelters, the dominant Hg output byproducts were similar, including waste acid, sulfuric acid, and cyanide leaching residue. Total Hg outputs from these three byproducts were 80% in smelter A and 84% in smelter B, which indicated that LSGP is a potential Hg release source in China. Waste acid was the largest Hg output in smelter A, which accounted for 33% of total Hg output. In smelter B, the proportion of Hg in the cyanide leaching residue reached 42%, much higher than the Hg proportion of 16% in the waste acid. Hg in the sulfuric acid took up 26% of total Hg outputs in both smelter A and smelter B. During the whole production processes, atmospheric Hg emissions accounted for 17% in smelter A and 10% in smelter B. Total atmospheric Hg emissions were 67 g/day in smelter A and 14 g/day in smelter B. Atmospheric Hg emissions from the roasting process was only 11 g/day and 4 g/day in smelters A and B, accounting for 16% and 29% of total atmospheric Hg emissions in the corresponding smelters.

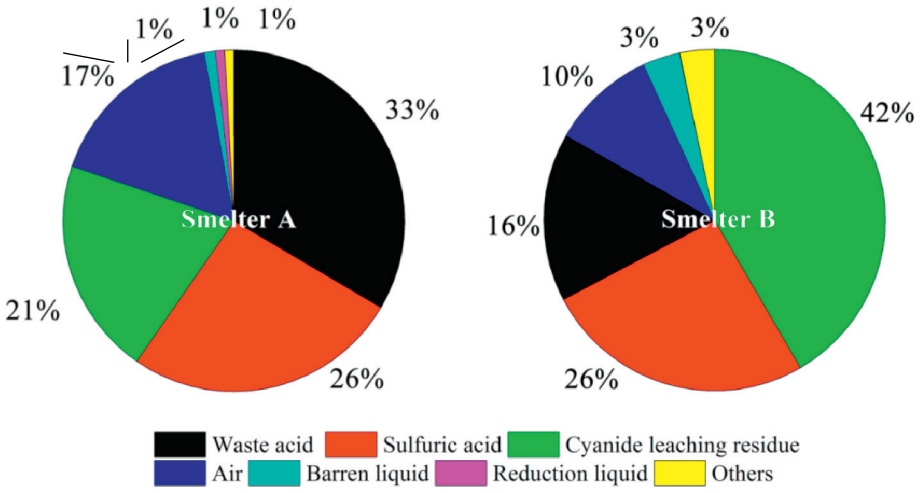

Fig. 3 – Overall Hg mass balances in the studied smelters.

2.4. Comparisons and implications

To compare with previous studies, Hg emission factors of tested smelters were calculated by the following equations.

$$ef_{LGSP} = ef_{roa} + ef_{ref} \quad (1)$$

$$ef_{roa} = \frac{E_{roa}}{C_{Au} \times M_{ore} \times \alpha} = \frac{C_{Hg} \times \gamma}{C_{Au} \times \alpha} \times (1-\eta_{APCDs}) \quad (2)$$

$$ef_{ref} = \frac{E_{ref}}{C_{Au} \times M_{ore} \times \alpha} = \frac{C_{Hg}}{C_{Au} \times \alpha} \times (1-\gamma+\gamma \times \eta_{DCs}) \times \theta_{Au-sludge} \times \theta_{ref-air} \quad (3)$$

where ef (kg/ton) is emission factor; $_{LGSP,\ roa,}$ and $_{ref}$ refer to the overall gold extraction process, roasting process and refining process, respectively. E (g/day) is atmospheric Hg emissions (see Fig. 1). C_{Au} (g/ton) and C_{Hg} (ng/g) are gold concentration and Hg concentration in the concentrates. The gold concentration in the concentrates was approximately 35 g/ton. M (ton/day) is concentrate consumption (Table 1); α is Au recovery rate during the overall gold extraction processes, 70%. γ (%) is Hg release rate in the roasting process. η (%) is Hg removal efficiency. $\theta_{Au\text{-}sludge}$ (%) is the proportion of Hg in the gold sludge in total Hg outputs to the cyanide leaching process (Fig. 1). $\theta_{ref\text{-}air}$ is the proportion of atmospheric Hg emissions in the total Hg output of the refining process (Fig. 1).

By using the above equations, the emission factors for the studied smelters were determined and are shown in Table 3. Emission factors for the whole processes were 9.6 kg/ton for smelter A and 7.6 kg/ton for smelter B. The tested emission factors were significantly lower than the derived emission factors applied in the emission inventories. The earlier emission factor of 790 kg/ton applied was derived from that for artisanal and small-scale gold mining, where emissions were much larger than the emissions from LGSP (Dai et al., 2003; Jiang, 2004; Streets et al., 2005; Wu et al., 2006). Thus, this

Table 3 – Hg emission factors for LSGP in different studies.

Processes	Emission factor (kg/ton)	Reference
Overall gold production processes	790*	Dai et al., 2003; Jiang, 2004; Streets et al., 2005; Wu et al., 2006
Overall gold production processes	500*	Pacyna et al., 2006; Pirrone et al., 2010
Overall gold production processes	25*	UNEP, 2005
Overall gold production processes	25–27*	AMAP/UNEP, 2008
Overall gold production processes	55*	AMAP/UNEP, 2013
Overall gold production processes	26*	Zhang et al., 2015; Pacyna et al., 2010
Overall gold production processes, changed with time	2–520*	Streets et al., 2011
Overall gold production processes, changed with time	28–72*	Wu et al., 2016
Overall gold production processes, changed with time	29–221*	Tian et al., 2015
Two-stage roasting process	0.5	Yang et al., 2016
Roasting processes	1.7	Gao et al., 2016
One-stage roasting process	2.2	This study
Two-stage roasting process	1.5	This study
Refining process	5.4–8.0	This study
Overall gold production processes	7.6–9.6	This study

LSGP: large-scale gold production.
* The emission factors were not obtained from field experiments.

emission factor was overestimated. Thereafter, the emission factor for LGSP was revised to 500 kg/ton (Pacyna et al., 2006; Pirrone et al., 2010). Later emission factors of 25–27 kg/ton were used in recent emission inventories (AMAP/UNEP, 2008; Pacyna et al., 2010; Zhang et al., 2015). These emission factors were further applied in the transformed normal distribution curve to generate year-by-year emission factors (Streets et al., 2011; Tian et al., 2015; Wu et al., 2016). However, during the revision process for emission factors, few field experiments were conducted to evaluate these emission factors. A recent field experiment in a LGSP indicated that the emission factor of the roasting process was 0.5–1.7 kg/ton (Yang et al., 2016; Gao et al., 2016), which was quite similar to our test result of 1.5 kg/ton. Thus, using the derived emission factors for inventory compilation may overestimate the atmospheric Hg emissions from current China's LGSP.

Hg flows in this study provided insight to compile a technology-based emission factor model for LGSP. However, the application of this model to LGSP still faced challenges. From Eqs. (1)–(3), the values of emission factors were impacted by many parameters, especially the Hg concentration in gold concentrates and the application situations of APCDs. Limited studies indicated that Hg concentrations in the gold concentrates varied over a wide range, from less than 0.1 ng/g to over 100,000 ng/g. Such a wide range of Hg concentrations would inevitably impact the estimation of Hg emissions from LGSP. Thus, Hg concentrations in gold concentrates require systematic investigation to reduce the uncertainty in the emission factor. In addition, China's current LGSP with roasting process have all installed FGS + ESD + APD for flue gas cleaning. However, these devices were not installed in early periods (*e.g.*, around 2000). To apply this model in compiling an historical emission inventory, the application situations of APCDs and gold extraction technologies require investigation. There have not been any relevant papers on the influence of matrix/impurities in the gold concentrates on the mercury emission factor so far. However, according to the study of the influence of coal components on mercury removal, the increase of Cl, Br, N, and S content will enhance the mercury oxidation ratio and decrease the mercury emission factor. The influence of matrix/impurities in the gold concentrates need to be further researched in the future.

Hg flows in the studied two smelters reflected Hg pollution control measures for China's LGSP, especially against the background of the implementation of the *Minamata Convention on Mercury*. If the tested average emission factor of 8.6 kg/ton (7.6–8.6 kg/ton) instead of 55 kg/ton were applied in the global Hg assessment report (AMAP/UNEP, 2013), atmospheric Hg emissions from China's LSGP would be only 2.0 ton. Compared to other significant emissions sources such as cement plants and coal-fired industrial boilers, Hg emission control in LSGP is not especially urgent currently. However, its contributions to China's emissions will increase when emission reduction is achieved in other significant emission sources. In the future, if emission control measures are to be applied in LSGP, more attention should be paid to emissions from the refining process. In addition, Hg concentrations in the flue gas of the refining process were as low as 4–6 $\mu g/m^3$, but the gas flow can reach 7200–12,000 km^3/day. Such concentration and operation parameters will add to the difficulty of Hg emission control from the refining process. Thus, development of technology for low-Hg flue gas but with large gas flow is needed currently to meet future control requirements. In addition, LSGP might be a potential Hg release source, and pollution from acid and sludge should be given attention.

3. Conclusions

A comprehensive investigation of Hg flows in the whole gold production process was carried out to identify the Hg emission points and to understand the Hg emission characteristics of LGSP. Hg input to LSGP was mainly from gold concentrates, and the dominant Hg output byproducts were waste acid, sulfuric acid, cyanide leaching residue and air. Overall atmospheric Hg emissions accounted for 17% in smelter A and 10% in smelter B of the corresponding Hg outputs. There were three dominant atmospheric Hg emission points in gold smelters, including the exhaust gas of the roasting process, exhaust gas from the environmental fog collection stack and exhaust gas from the converter of the refining process. Atmospheric Hg emissions from the roasting process only accounted for 16% and 29% of total Hg emissions in smelter A and smelter B. Most of the atmospheric Hg was emitted from the refining process. When atmospheric Hg emissions from both the roasting and refining processes were considered, the overall Hg speciation profile ($Hg^0/Hg^{2+}/Hg_p$) for LSGP was 34.1/57.1/8.8, which was quite different from the derived profile of 80/15/5 applied in previous emission inventories of LSGP. Overall emission factors were 9.6 kg/ton for smelter A and 7.6 kg/ton for smelter B, which were much lower than previous emission factors applied due to the high synergistic Hg removal efficiency of APCDs in the roasting process. Thus, using the derived emission factors for inventory compilation may overestimate the atmospheric Hg emissions from China's current LGSP. Atmospheric Hg emission control in LSGP is not especially urgent currently in China. In the future, if emission control measures are to be applied in LSGP, more attention should be paid to emissions from the refining process. Currently, development of technology on low-Hg flue gas but with large gas flow is needed to meet future control requirements. LSGP might be a potential Hg release source and pollution from acid and sludge should be given attention.

Acknowledgments

This study was supported by the National basic Research Program (973) of China (No. 2013CB430001), the National Natural Science Foundation of China (No. 21077065), and the China Postdoctoral Science Foundation (2016T90103, 2016M601053).

REFERENCES

AMAP/UNEP, 2008. Arctic Monitoring and Assessment Programme and United Nations Environment Programme. Technical Background Report for the Global Mercury Assessment. AMAP/UNEP, Geneva, Switzerland.

AMAP/UNEP (Arctic Monitoring and Assessment Programme and United Nations Environment Programme), 2013. Technical Background Report for the Global Mercury Assessment. AMAP/UNEP, Geneva, Switzerland.

ASTM (American Society for Testing and Materials), 2002. Technical Background Report for the Global Mercury Assessment. Particle-Bound and Total Mercury in Flue Gas Generated from Coal-Fired Stationary Sources (Ontario Hydro Method). ASTM, Pennsylvania, United States.

CGS (China Gold Association), 2015. China Gold Yearbook. CGS, Beijing, China.

Dai, Q., Feng, X.B., Qiu, G.L., Jiang, H.C., 2003. Mercury contaminations from gold mining using amalgamation technique in Xiaoqinling region, Shanxi Province, PR China. J. Phys. Paris 7, 4.

Gao, J.J., Yue, T., Zuo, P.L., Liu, Y., Tong, L., Wang, C.L., et al., 2016. Current status and atmospheric mercury emissions associated with large-scale gold smelting industry in China. Aerosol Air Qual. Res.

GAQSIQ, 2014. (General Administration of Quality Supervision Inspection and Quarantine of the People 's Republic of China) Sulfuric acid. China Standardization Publisher, Beijing, China.

Jiang, J.K., 2004. Preliminary studies on emission and control of atmospheric mercury in China. Vol. Master Tsinghua University, School of Environment, Beijing, China 117.

MEP (Ministry of the Environment), 2002. Technical Specifications Requirements for Monitoring of Surface Water and Waste Water (HJ/T 91-2002). Beijing, China.

Pacyna, E.G., Pacyna, J.M., Steenhuisen, F., Wilson, S., 2006. Global anthropogenic mercury emission inventory for 2000. Atmos. Environ. 40, 4048–4063.

Pacyna, E.G., Pacyna, J.M., Sundseth, K., Munthe, J., Kindbom, K., Wilson, S., et al., 2010. Global emission of mercury to the atmosphere from anthropogenic sources in 2005 and projections to 2020. Atmos. Environ. 44, 2487–2499.

Pirrone, N., Chinirella, S., Feng, X.B., Finkelman, R.B., Friedli, H.R., Leaner, J., et al., 2010. Global mercury emissions to the atmosphere from anthropogenic and natural sources. Atmos. Chem. Phys. 10, 5951–5964.

Streets, D.G., Devane, M.K., Lu, Z.F., Bond, T.C., Sunderland, E.M., Jacob, D.J., 2011. All-time releases of mercury to the atmosphere from human activities. Environ. Sci. Technol. 45, 10485–10491.

Streets, D.G., Hao, J.M., Wu, Y., Jiang, J.K., Chan, M., Tian, H.Z., et al., 2005. Anthropogenic mercury emissions in China. Atmos. Environ. 39, 7789–7806.

Tian, H.Z., Zhu, C.Y., Gao, J.J., Cheng, K., Hao, J.M., Wang, K., et al., 2015. Quantitative assessment of atmospheric emissions of toxic heavy metals from anthropogenic sources in China: historical trend, spatial distribution, uncertainties, and control policies. Atmos. Chem. Phys. 15, 10127–10147.

UNEP (United Nations Environment Programme), 2005. Toolkit for identification and quantification of mercury release Geneva,Switzerland.

UNEP (United Nations Environment Programme), 2013a. Minamata Convention on Mercury. UNEP, Minamata, Japan.

UNEP (United Nations Environment Programme), 2013b. Toolkit for identification and quantification of mercury releases. Guideline for Inventory Level 2, Version 1.3. UNEP, Geneva, Switzerland.

US EPA (United States Environmental Protection Agency), 1994. Method 7470a: Hg in liquid waste (manual cold-vapor technique). US EPA, Washinton D. C., United States.

US EPA (United States Environmental Protection Agency), 1998. Method 7473: Hg in sSolids and sSolutions by ThermaldDecomposition Amalgamation and Atomic Absorption Spectrophotometry. US EPA, Washinton D. C., United States.

Wang, F.Y., Wang, S.X., Zhang, L., Yang, H., Gao, W., Wu, Q.R., et al., 2016. Mercury mass flow in iron and steel production process and its implications for mercury emission control. J. Environ. Sci. 43, 293–301.

Wu, Q.R., Wang, S.X., Hui, M.L., Wang, F.Y., Zhang, L., Duan, L., et al., 2015a. New insight into atmospheric mercury emissions from zinc smelters using mass flow analysis. Environ. Sci. Technol. 49, 3532–3539.

Wu, Q.R., Wang, S.X., Hui, M.L., Wang, F.Y., Zhang, L., Duan, L., et al., 2015b. New insight into atmospheric mercury emissions from zinc smelters using mass flow analysis. Environ. Sci. Technol. 49, 3532–3539.

Wu, Q.R., Wang, S.X., Li, G.L., Liang, S., Lin, C.-J., Wang, Y.F., et al., 2016. Temporal Trend and Spatial Distribution of Speciated Atmospheric Mercury Emissions in China During 1978–2014. Environ. Sci. Technol. 50, 13428–13435.

Wu, Y., Wang, S.X., Streets, D.G., Hao, J.M., Chan, M., Jiang, J.K., 2006. Trends in anthropogenic mercury emissions in China from 1995 to 2003. Environ. Sci. Technol. 40, 5312–5318.

Yang, M., Wang, S.X., Zhang, L., Wu, Q.R., Wang, F.Y., Hui, M.L., et al., 2016. Mercury emission and speciation from industrial gold production using roasting process. J. Geochem. Explor. 170, 72–77.

Zhang, L., Wang, S.X., Meng, Y., Hao, J.M., 2012a. Influence of mercury and chlorine content of coal on mercury emissions from coal-fired power plants in China. Environ. Sci. Technol. 46, 6385–6392.

Zhang, L., Wang, S.X., Wang, L., Wu, Y., Duan, L., Wu, Q.R., et al., 2015. Updated emission inventories for speciated atmospheric mercury from anthropogenic sources in China. Environ. Sci. Technol. 49, 3185–3194.

Zhang, L., Wang, S.X., Wu, Q.R., Meng, Y., Yang, H., Wang, F.Y., et al., 2012b. Were mercury emission factors for Chinese non-ferrous metal smelters overestimated? Evidence from onsite measurements in six smelters. Environ. Pollut. 171, 109–117.